Inorganic Chemistry

Communication

pubs.acs.org/IC

Novel Lithium-Containing Honeycomb Structures

Vinod Kumar, Neha Bhardwaj, Nobel Tomar, Vaishali Thakral, and S. Uma*

Materials Chemistry Group, Department of Chemistry, University of Delhi, Delhi, India

Supporting Information

ABSTRACT: Rock-salt-based honeycomb structures containing Te^{VI} and Sb^{V} with innumerable prospects of properties and applications were realized in the two new series of mixed-metal oxides of lithium, $Li_8M_2Te_2O_{12}$ (M^{II} = Co, Ni, Cu, Zn) and $Li_8M_2Sb_2O_{12}$ (M^{III} = Cr, Fe, Al, Ga). The structures of $Li_8Co_2Te_2O_{12}$ and $Li_8Cu_2Te_2O_{12}$ were determined by single-crystal X-ray diffraction for the first time, and mixed-occupancy Li/M was identified.

Among several of the known inorganic functional materials, specifically oxides play a major role over others because of their higher stability and synthetic accessibility by various methods. In particular, the family of mixed-metal oxides with brucite-like octahedral layers that are separated and charge-compensated by alkali-metal ions (Li^+, Na^+, or K^+) have continued to attract the attention of several researchers. Some of the simplest oxides such as $LiCoO_2$ and $LiMnO_2$ are excellent electrode materials for Li-ion batteries.[1] Studies involving P2-Na_xCoO_2 ($x \leq 1$)[2] phases along with the hydrate[3] have been the subject of a thorough investigation for thermoelectric applications and interesting superconductivity behavior, respectively. A variety of oxides with a wide range of structures and properties can be obtained depending upon the nature of the alkali-metal ions (Li^+, Na^+, or K^+) and also by the introduction of additional metal ions in the octahedral layers. The rationale behind the investigation of these mixed-metal oxides by the systematic variation of the cations can be categorically reasoned. The primary focus has been the structural diversity achieved by the synthetic solid-state exploration ranging from the ordered NaCl variants[4] (e.g., α-$NaFeO_2$) to their ordered superstructure variants such as $Li_3M_2XO_6$ (M = Mg, Co, Ni, Cu; X = Nb, Ta, Sb) and $Na_3M_2XO_6$ (M = Mg, Co, Ni, Cu, Zn; X = Sb) possessing honeycomb lattices.[5,6] Furthermore, layered oxides with varying transition-metal stacking of octahedral layers[7] are possible in $A_2MX_2O_6$ (A = Li, Na; M = Ni, Mg; X = Mn, Ti).

An additional advantage of this material expansion would be the identification of possible cathode materials for Li-ion batteries (e.g., $Li_3Ni_2SbO_6$,[8] $Li_3Mn_2SbO_6$[9]). The best scientific interest that can be considered next along this line is proportional to the mobility of the interlayer alkali-metal ions and thus responsible for the discovery of novel ionic conductors, namely, $Li_3Zn_2SbO_6$[10] and $Na_2M_2TeO_6$ (M = Ni, Co, Zn, Mg).[11] As a consequence, soft chemical ion-exchange methods can be used to replace the alkali-metal ions with cations such as Ag^+, for example, in order to yield potential visible-light photocatalysts[12] (e.g., Ag_2TiO_3, Ag_2SnO_3) and/or materials relevant to transparent conductors[13] (e.g., $Ag_3Ni_2SbO_6$). Yet another fascination has been the presence of magnetic metal ions in the honeycomb arrays and, hence, leads to the study of the important phenomenon of physics involving the occurrence of strong magnetic fluctuation and spin-gap behavior. Li_2RuO_3 with alternating close-packed layers of Li and $LiRu_2$ undergoes a metal−insulator transition accompanied by the appearance of a spin gap below 600 K.[14] The structure of the corresponding $Ag_3LiRu_2O_6$ preserved the Li/Ru order in the honeycomb layers and was suggested to be a potential thermoelectric material based on its excellent electrical conductivity (0.01 Ω cm^{-1}) at room temperature.[15] The spin-gap behavior of $Na_3Cu_2SbO_6$,[16] $Li_3Cu_2SbO_6$,[5] and $Na_2Cu_2TeO_6$[17] oxides, and the low-temperature magnetic ordering[18] in $Na_2Co_2TeO_6$ and $Na_3Co_2SbO_6$ have been investigated in detail.

Nalbandyan and co-workers over the past decade have identified several of the above oxides.[6,9,11,19,20] Subramanian et al.[21] reported the ordering of Ni^{2+} and Bi^{5+} ions in the oxides $Li_3Ni_2BiO_6$ and $Li_3NiMBiO_6$ (M = Mg, Cu, Zn) and characterized the electrochemical behavior of $Li_3Ni_2BiO_6$ as a cathode material. The surprisingly broader material aspect of these oxides prompted us to synthesize new honeycomb-ordered structures by suitable cationic variations and to identify the cationic ordering by structural investigation. Herein, we report the synthesis and characterization of two new series of mixed-metal oxides of lithium, $Li_8M_2Te_2O_{12}$ (M^{II} = Co, Ni, Cu, Zn) and $Li_8M_2Sb_2O_{12}$ (M^{III} = Cr, Fe, Al, Ga) containing Te^{VI} and Sb^{V} ions, respectively. The structures have been confirmed by the powder X-ray diffraction (PXRD) of the polycrystalline samples and by single-crystal X-ray diffraction (SCXRD) studies of $Li_8Co_2Te_2O_{12}$ and $Li_8Cu_2Te_2O_{12}$.

A comparison of the structure of $Na_2Cu_2TeO_6$[17] (Figure S1 in the Supporting Information) and that of oxides such as $Na_3Cu_2SbO_6$[18] and $Li_3Ni_2SbO_6$[19] (Table S1 in the SI), clearly distinguished the additional Na^+/Li^+ ions in the octahedral intercalation sites[22] of the latter. We envisaged the possibilities of (i) synthesizing the lithium analogue of $Na_2Cu_2TeO_6$ and (ii) introducing additional Li atoms while appropriately balancing the cationic stoichiometry. Conventional solid-state methods were adopted for the synthesis, and homogenized stoichiometries $Li_3Cu_{2.25}Te_{0.75}O_6$ and $Li_2Cu_2TeO_6$ using high-purity reactants were calcined between 650 °C and 800 °C for 12−24 h (SI). The PXRD patterns of the products suggested the presence of a monoclinic layer structure. Subsequently, single crystals were grown by melting the above compositions (SI). The SCXRD solution for the crystal obtained (I) from the melt of $Li_3Cu_{2.25}Te_{0.75}O_6$ was carried out in the space group

Received: May 30, 2012
Published: October 4, 2012

   dx.doi.org/10.1021/ic301125n | *Inorg. Chem.* 2012, 51, 10471−10473

*C*2/*m*, with the initial model comprising one of each of the Te, Cu, and Li atoms along with two O atoms in the 2a, 4g, 4h, 8j, and 4i sites, respectively. The difference Fourier map showed additional electron density at the 2d site and the refinement satisfactorily converged by the introduction of both Li and Cu atoms at this site. Verification of the occupancies of both Li2/Cu2 and Li3/Cu3 at the 2d and 4g sites resulted in Li2 and Li3 to 0.32(1) and 0.85(1), respectively, and the stoichiometry was found to be $(Li_4(Li_{0.64(1)}Cu_{1.36(1)}))(Li_{3.40(1)}Cu_{0.60(1)}Te_2)O_{12}$. The final crystallographic parameters, the positional and thermal parameters are listed (Tables S2 and S3 in the SI). The PXRD pattern (Figure 1A) of the sample synthesized from

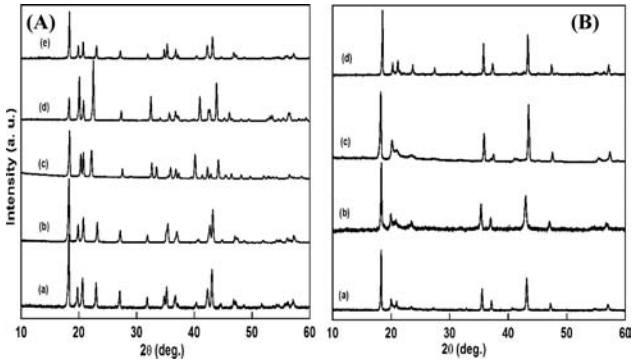

Figure 1. (A) PXRD patterns of (a) $Li_8Co_2Te_2O_{12}$, (b) $Li_8Ni_2Te_2O_{12}$, (c) $Li_{7.40}Cu_{2.72}Te_{1.88}O_{12}$, (d) $Li_8Cu_2Te_2O_{12}$, and (e) $Li_8Zn_2Te_2O_{12}$. (B) PXRD patterns of $Li_8M_2Sb_2O_{12}$ with M^{III} as (a) Cr, (b) Fe, (c) Al, and (d) Ga.

$Li_8Cu_2Te_2O_{12}$ composition confirmed the single-phase formation and stoichiometry (Figure S2 in the SI). The crystal structure is different from that of $Na_2Cu_2TeO_6$, wherein only one type of Na fills the voids between the infinite honeycomb layers formed by the ordering of Te and Cu (Figure S1 in the SI). The structure of $Li_8Cu_2Te_2O_{12}$ of the present study rather resembled $Li_3Ni_2SbO_6$ but with a mixed Li/Cu occupancy. The honeycomb layer formed by the ordering of Te1 and Li3/Cu3 ions (Table S3 in the SI and Figure 2A). The TeO_6 octahedra

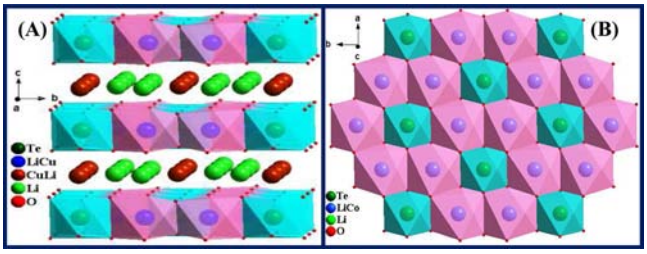

Figure 2. Crystal structures of (A) $Li_8Cu_2Te_2O_{12}$ in a view perpendicular to the edge-shared honeycomb layers and (B) $Li_8Co_2Te_2O_{12}$ showing the honeycomb array of edge-shared MO_6 octahedra.

are almost regular, with Te−O bonds ranging between 1.91 and 1.94 Å, and match well with the bond lengths expected for Te^{VI}-based oxides.[11,17] Each of these TeO_6 shares the edges with the distorted $(Li3/Cu3)O_6$ octahedron, with bond lengths varying between 2.06 and 2.23 Å (Table S4 in the SI). Finally, the voids between these layers have one more Li2/Cu2 ion (reddish-brown spheres in Figure 2A), in addition to the Li1 (green spheres in Figure 2A) site. A similar case of mixed occupancy (Li/Cu) was reported only in the case of $Li_3Cu_2SbO_6$.[5] The structure with interleaving Li and Li/Cu ions in $Li_8Cu_2Te_2O_{12}$ is evident from its inability to undergo complete ion (Ag^+)-exchange reactions. The option of having Li^+ ions within the slabs gives rise to the possibility of combining various M^{II} (e.g., Co, Ni, Cu, Zn) or M^{III} (e.g., Fe, Cr, Al, Ga) ions respectively with Te^{VI} and Sb^V ions.

Thus, we explored the synthesis of other members of the series $Li_8M_2Te_2O_{12}$ (M^{II} = Co, Ni, Zn), and the PXRD patterns (Figure 1A) confirmed the formation of single phases. The Le Bail fit of the PXRD patterns of $Li_8Ni_2Te_2O_{12}$ and $Li_8Zn_2Te_2O_{12}$ (Figure S2 in the SI) could be matched using the monoclinic lattice (space group *C*2/*m*) parameters (Table 1). In the case of $Li_8Co_2Te_2O_{12}$, although the single-crystal structure solution (Table S3 in the SI) established the overall stoichiometry, differences prevailed in the distribution of the Li and Co atoms in the various crystallographic sites [i.e., $Li_6(Li_2Co_2Te_2)O_{12}$]. A successful convergence (R_1 = 2.01%) was achieved with Li1 in 4h, Li2 in 2d and a mixed Li/Co at the 4g sites (Figure S1 in SI). The selected bond distances are given in Table S4 in the SI. The honeycomb array consisting of edge-sharing $(Li/Co)O_6$ and TeO_6 octahedra is shown in Figure 2B. The room temperature field-dependent magnetization (Figure 3A) suggested a paramagnetic behavior for Co^{2+} ions. Surprisingly, the SCXRD data obtained (II) from the $Li_2Cu_2TeO_6$ composition was found to be $Li_{7.40}Cu_{2.72}Te_{1.88}O_{12}$ (Table S2 and S3 in the SI). The structures of I and II are expected to be similar because of the close reactant stoichiometry. However, the solution from direct methods, after appropriate least-squares refinements, yielded $(Li_4(Li_{1.36(1)}Cu_{0.64(1)}))(Li_{2.04(1)}Cu_{1.96(1)}Te_{1.88(3)}Cu_{0.06(3)})O_{12}$. Differences were in the Li2/Cu2 distribution at the 2d site, 0.32 Li in I versus 0.68 in II, and in the Li3/Cu3 distribution at the 4g site, 0.85 Li in I versus 0.51 in II (Table S3 in the SI). The overall differences include the presence Cu (0.06) at the Te (2a) site in II and, the variation in the Li/Cu distribution led to the formation of I and II. Structurally, this means that the amounts of Li and, hence, Cu present in the interlayer as well as in the octahedral slabs are changed in I and II (Figure 2A) and are evident from the variation observed in the intensities of the reflections occurring at $15° \leq 2\theta \leq 25°$ in the PXRD patterns (Figure 1A). Interestingly, the two oxides showed different behaviors in their field-dependent magnetization at room temperature (Figure 3A). Almost a simple paramagnetic behavior was observed in $Li_{7.40}Cu_{2.72}Te_{1.88}O_{12}$, and a magnetic-field-dependent transition was noticed in $Li_8Cu_2Te_2O_{12}$ without the presence of a significant hysteresis loop. The possibility of such a spin-flop transition was reported[18] in $Na_3Co_2SbO_6$ based on the low-temperature magnetization behavior. The role played by the compositional range of Li along with that of Cu in the formation of I and II and their temperature dependent magnetization behavior are currently being investigated. As noted earlier, the presence of Li^+ ions within the slabs offers the unique possibility of substituting trivalent (M^{III} = Fe, Cr, Al, Ga) ions in combination with Sb^{5+} ions. Accordingly, we could synthesize the oxides represented by the series $Li_6(Li_2M_2Sb_2)O_{12}$ (M^{III} = Fe, Cr, Al, Ga). The monoclinic lattice parameters (Table 1) derived from the PXRD patterns (Figure 1B) revealed the formation of layered structures with stacking faults (Figure S3 in the SI).

The ion mobility, especially of lithium in the metal oxides, is measurable by the ionic conductivity and ion-exchange

dx.doi.org/10.1021/ic301125n | *Inorg. Chem.* 2012, 51, 10471−10473

Table 1. Cell Parameters (Space Group $C2/m$) of the Honeycomb Structures Obtained from PXRD

compound	a (Å)	b (Å)	c (Å)	β (deg)
$Li_8Co_2Te_2O_{12}$	5.198(2)	8.906(3)	5.145(1)	110.636(5)
$Li_8Ni_2Te_2O_{12}$	5.1603(3)	8.8914(5)	5.1426(4)	110.209(3)
$Li_{7.40}Cu_{2.72}Te_{1.88}O_{12}$	5.3916(3)	8.7359(5)	5.3059(3)	114.531(3)
$Li_8Cu_2Te_2O_{12}$	5.268(1)	8.773(2)	5.231(1)	113.281(2)
$Li_8Zn_2Te_2O_{12}$	5.2216(3)	8.9279(6)	5.1683(3)	110.827(5)
$Li_8Cr_2Sb_2O_{12}$	5.1232(3)	8.8555(5)	5.1316(3)	109.464(7)
$Li_8Fe_2Sb_2O_{12}$	5.1643(4)	8.916(1)	5.1599(5)	109.478(9)
$Li_8Al_2Sb_2O_{12}$	5.068(14)	8.769(24)	5.136(14)	109.309(14)
$Li_8Ga_2Sb_2O_{12}$	5.1349(2)	8.8746(6)	5.1554(4)	109.376(4)

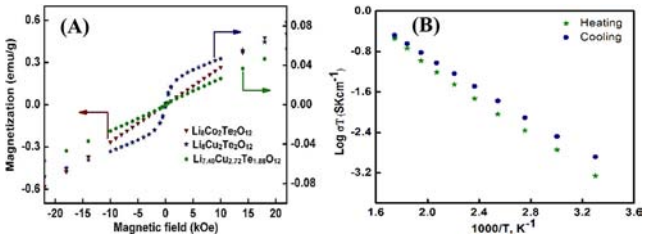

Figure 3. (A) Plot of magnetization versus magnetic field and (B) Arrhenius plots for total (ac) conductivity of $Li_8Co_2Te_2O_{12}$.

reactions, and the latter has been useful in synthesizing oxides that are otherwise inaccessible by the usual solid-state methods.[23] By molten ion exchange with $AgNO_3$, oxides such as $Ag_6(Li_2M_2^{II}Te_2)O_{12}$ (M^{II} = Co, Ni, Zn) and $Ag_6(Li_2M_2^{III}Sb_2)O_{12}$ (M^{III} = Cr, Fe, Al, Ga; Figures S4 and S5 in the SI) were synthesized. The ionic conductivity of $Li_8Co_2Te_2O_{12}$ showed temperature dependence obeying the Arrhenius law with an activation energy of 0.28(2) eV (Figure 3B).

■ ASSOCIATED CONTENT

Supporting Information

Synthesis, characterization, single-crystal structure determination, other crystallographic data, and PXRD patterns. This material is available free of charge via the Internet at http://pubs.acs.org.

■ AUTHOR INFORMATION

Corresponding Author

*E-mail: suma@chemistry.du.ac.in.

Notes

The authors declare no competing financial interest.

■ ACKNOWLEDGMENTS

This work was supported by the DST, Government of India, and University of Delhi (DU). We thank the USIC and M. Tech. Nanoscience, DU, for the XRD facilities. We thank Dr. R. Nagarajan for constant support. V.K. and N.B. thank the CSIR, and V.T. thanks UGC for SRF.

■ REFERENCES

(1) Whittingham, M. S. *Mater. Res. Bull.* **2008**, *33*, 411. Goodenough, J. B.; Kim, Y. *Chem. Mater.* **2010**, *22*, 587. Huggins, R. A. *Advanced Batteries, Materials Science Aspects*; Springer: New York, 2009.

(2) Molenda, J.; Delmas, C.; Hagenmuller, P. *Solid State Ionics* **1983**, *9 − 10*, 431. Molenda, J.; Delmas, C.; Dordor, P.; Stokłosa, A. *Solid State Ionics* **1989**, *12*, 473.

(3) Lee, M.; Viciu, L.; Li, L.; Wang, Y.; Foo, M. L.; Watauchi, S.; Pascal, R. A., Jr.; Cava, R. J.; Ong, N. P. *Nat. Mater.* **2006**, *5*, 537. Takada, K.; Sakurai, H.; Takayama-Muromachi, E.; Izumi, F.; Dilanian, R. A.; Sasaki, T. *Nature* **2003**, *422*, 53.

(4) Delmas, C.; Braconnier, J. J.; Maazaz, A.; Hagenmuller, P. *Rev. Chim. Minér.* **1982**, *19*, 343. Delmas, C.; Maazaz, A.; Fouassier, C.; Reauet, J. M.; Hagenmuller, P. *Mater. Res. Bull.* **1979**, *14*, 329.

(5) Mather, G. C.; Smith, R. I.; Skakle, J. M. S.; Fletcher, J. G.; Castellanos, R. M. A.; Gutierrez, M. P.; West, A. R. *J. Mater. Chem.* **1995**, *5*, 1177. Skakle, J. M. S.; Castellanos, R. M. A.; Tovar, S. T.; West, A. R. *J. Solid State Chem.* **1997**, *131*, 115. Mather, G. C.; West, A. R. *J. Solid State Chem.* **1996**, *124*, 214.

(6) Smirnova, O. A.; Nalbandyan, V. B.; Petrenko, A. A.; Avdeev, M. *J. Solid State Chem.* **2005**, *178*, 1165. Politaev, V. V.; Nalbandyan, V. B.; Petrenko, A. A.; Shukaev, I. L.; Volotchaev, V. A.; Medvedev, B. S. *J. Solid State Chem.* **2010**, *183*, 684.

(7) Paulsen, J. M.; Donaberger, R. A.; Dahn, J. R. *Chem. Mater.* **2000**, *12*, 2257.

(8) Ma, X.; Kang, K.; Ceder, G.; Meng, Y. S. *J. Power Sources* **2007**, *173*, 550.

(9) Pospelov, A. A.; Nalbandyan, V. B.; Serikova, E. I.; Medvedev, B. S.; Evstigneeva, M. A.; Ni, E. V.; Lukov, V. V. *Solid State Sci.* **2011**, *13*, 1931.

(10) Greaves, C.; Katib, S. M. A. *Mater. Res. Bull.* **1990**, *25*, 1175.

(11) Evstigneeva, M. A.; Nalbandyan, V. B.; Petrenko, A. A.; Medvedev, B. S.; Kataev, A. A. *Chem. Mater.* **2011**, *23*, 1174.

(12) Hosogi, Y.; Kato, H.; Kudo, A. *J. Mater. Chem.* **2008**, *18*, 647.

(13) Nagarajan, R.; Uma, S.; Jayaraj, M. K.; Tate, J.; Sleight, A. W. *Solid State Sci.* **2002**, *4*, 787.

(14) James, A. C. W. P.; Goodenough, J. B. *J. Solid State Chem.* **1988**, *74*, 287. Miura, Y.; Yasui, Y.; Sato, M.; Igawa, N.; Kakurai, K. *J. Phys. Soc. Jpn.* **2007**, *76*, 033705.

(15) Kimber, S. A. J.; Ling, C. D.; Morris, D. J. P.; Chemseddine, A.; Henry, P. F.; Argyriou, D. N. *J. Mater. Chem.* **2010**, *20*, 8021.

(16) Miura, Y.; Hirai, R.; Fujita, T.; Kobayashi, Y.; Sato, M. *J. Magn. Magn. Mater.* **2007**, *310*, 389.

(17) Xu, J.; Assoud, A.; Soheilnia, N.; Derakhshan, S.; Cuthbert, H. L.; Greedan, J. E.; Whangbo, M. H.; Kleinke, H. *Inorg. Chem.* **2005**, *44*, 5042.

(18) Viciu, L.; Huang, Q.; Morosan, E.; Zandbergen, H. W.; Greenbaum, N. I.; McQueen, T.; Cava, R. J. *J. Solid State Chem.* **2007**, *180*, 1060.

(19) Zvereva, E. A.; Evstigneeva, M. A.; Nalbandyan, V. B.; Savelieva, O. A.; Ibragimov, S. A.; Volkova, O. S.; Medvedeva, L. I.; Vasiliev, A. N.; Klingeler, R.; Buechner, B. *Dalton Trans.* **2012**, *41*, 572.

(20) Nalbandyan, V. B.; Shukaev, I. L. *Russ. J. Inorg. Chem.* **1992**, *37*, 1231. Shukaev, I. L.; Volochaev, V. A. *Russ. J. Inorg. Chem.* **1995**, *40*, 1974. Smirnova, O. A.; Nalbandyan, V. B.; Avdeer, M.; Medredera, L. I.; Medvedev, B. S.; Kharton, V. V.; Marques, F. M. B. *J. Solid State Chem.* **2005**, *178*, 172.

(21) Berthelot, R.; Schmidt, W.; Muir, S.; Eilertsen, J.; Etienne, L.; Sleight, A. W.; Subramanian, M. A. *Inorg. Chem.* **2012**, *51*, 5377.

(22) Delams, C.; Fouassier, C.; Hagenmuller, P. *Physica B+C* **1980**, *99*, 81.

(23) Sebastian, L.; Gopalakrishnan, J. *J. Mater. Chem.* **2003**, *13*, 433. Nalbandyan, V. B. *J. Solid State Electrochem.* **2011**, *15*, 891.